Diffraction by Lossy Dielectric Wedges Using Both Heuristic UTD Formulations and FDTD

Jean-François Rouviere, Nicolas Douchin, and Paul F. Combes

***Abstract*—An improvement of the uniform theory of diffraction (UTD) coefficient for the case of a lossy dielectric wedge when a transmitted ray exists is presented. We elaborated two new terms that are added to the classical UTD diffraction coefficient, so that we obtain continuity of the total field. This new UTD formulation is compared to a numerical method based on finite difference time domain (FDTD). We outline the adaptation of the FDTD grid calculation, which was necessary to isolate only one edge diffraction and to treat two-dimensional (2-D) structures with two infinite sides. This comparison allows one to conclude that the new diffraction coefficient is relevant for the case of a lossy dielectric wedge. Then we present a comparison between two different versions of the UTD diffraction coefficient based on single or multiple reflection in the case of a dielectric slab. Thus, we can conclude to the significance of the multipaths for modeling dielectric structures. Finally, we analyze the results obtained with two consecutive wedge vertices in order to show that the slope diffraction related to the doubly diffracted field allows one to predict the field behind the structure when the transmitted field doesn't exist.**

***Index Terms*—Electromagnetic diffraction, FDTD, geometrical theory of diffraction, lossy media, wedges.**

I. Introduction

With the expansion of mobile cellular communications there is a need for more and more precise and general radiowave propagation models. Moreover, the large dimension of objects in relation to the wavelength and the possibility to repeat propagation calculation as often as possible in a limited computation time lead to the use of high-frequency asymptotic methods based on the ray concept, among which are the geometrical theory of diffraction (GTD) and its extension the uniform theory of diffraction (UTD) [1]. These techniques allow one to compute reflection and diffraction effects that are the dominant mechanisms in an urban environment.

The state of the art shows that these asymptotic wedge diffraction methods were derived rigorously for perfectly conducting infinite wedges or impedance wedges [2]–[4], but only heuristic extensions have been proposed to handle dielectric wedges as well as finite size ones. Several authors [5]–[7] propose heuristic approaches in the case of dielectric structures. In [5], the study is limited to a dielectric slab. In this case, the shadow boundary related to the transmitted rays is exactly the same as the incident shadow boundary (ISB). Furthermore, the validity of the approach is not completely verified. Indeed, the comparison between UTD and the moment method (MM) is made only in the case of the backward scattering half-plane directions and the calculation is not performed when transmitter and receiver are located on each side of the slab. Luebbers also studied dielectric structures: first in the case of knife edges and great size wedges [6], but without taking into account the transmitted field; then in the case of rough lossy wedges [7], he developed a heuristic UTD slope diffraction valid for diffraction over consecutive wedge faces when transmission through the wedge can be neglected. Nevertheless, in [6] and [7], no comparison with an exact method [MM or finite difference time domain (FDTD)] is presented.

Basically, materials used in urban environment are lossy dielectrics and the set of scatterers encountered during a ray path may include objects that cannot be considered infinite in comparison to the wavelengths commonly used (30 cm). Hence, there is a need to evaluate precisely the validity domain and the accuracy of these extended asymptotic methods by comparing them to exact approaches such as the FDTD.

In Section II, we report on the implementation of UTD in the case of a lossy dielectric wedges including an extra transmission coefficient. We propose a new approach to deal with the two-dimensional (2-D) problem of the diffraction by a lossy dielectric wedge. In case transmitted rays exist, the classic UTD formulation with the four-terms diffraction coefficient cannot compensate the discontinuity caused by the transmitted field on the transmission shadow boundary (TSB). Thus, we built up an improved formulation of the diffraction coefficient in which appear two additional terms weighted by the transmission coefficients of each dielectric interface. Thus, the total field depending on a six-terms diffraction coefficient is perfectly continuous whatever the incidence and the polarization of the incident wave.

Then, in Section III, we compare the results obtained with these asymptotic methods to those obtained with an exact method (FDTD) in the case of a single wedge such as in [8], where Stratis *et al.* use FDTD to obtain numerical diffraction coefficients for generic infinite perfectly electrically conducting (PEC), lossless, and lossy dielectric wedges. In this section, we outline the adaptation needed to the classic FDTD grid calculation to isolate only one edge diffraction and then validate FDTD on a metallic case by comparing with UTD. Results obtained in the dielectric case are also presented.

Even though good results have been obtained in application of the six-terms UTD diffraction coefficient, some differences remain as soon as we penetrate inside the shadow area. Since

Manuscript received June 30, 1997; revised June 10, 1999. This work was supported by FRANCE-TELECOM/CNET.

The authors are with ONERA/CERT/DERMO, Toulouse Cedex, F-31055 France.

Publisher Item Identifier S 0018-926X(99)09949-4.

0018–926X/99$10.00 © 1999 IEEE

in this zone it only exists diffracted and transmitted fields we think that we could improve the results by taking into account multiple reflections and transmission. As the case of the wedge is quite difficult to implement in UTD, in Section IV, we compare both single and multiple reflection formulations in the case of a dielectric slab. We obtain a good agreement between UTD and FDTD, which could explain that the differences obtained in the case of the dielectric wedge are due to the fact that multiple reflections are not taken into account in this case. In Section V, we also demonstrate how the double diffraction coefficient can improve the results obtained with UTD when multiple reflections are not included in the calculation.

II. Improvement of the UTD Diffraction Coefficient by Adding Two New Terms

The problem of the diffraction of an electromagnetic incident wave by a metallic or dielectric edge (Fig. 1) is an important canonical case in the frame of propagation studies in urban environment when modeling radio communications links with mobiles. The UTD is an asymptotic ray method which is well known for its fast computation time, but only rigorously established for perfectly conducting wedges. The originality of our work consists in the improvement of the diffraction coefficient for the case of diffraction by a wedge made of a lossy dielectric material such as concrete ($\epsilon_r = 10, \sigma = 0.001$ S/m). If the apex angle of the wedge is small enough ($\alpha < 20°$) a transmitted ray exists across the wedge from a new shadow boundary called transmitted shadow boundary (TSB) [9]. For an incident wave on the o face, the space around the wedge can be split into four areas limited by the incident shadow boundary (ISB_o), the reflected shadow boundary (RSB_o), and the TSB_o. In each area the following fields exist (Fig. 1):

Zone I $U_{\text{total}} = U_{\text{reflected}} + U_{\text{incident}} + U_{\text{diffracted}}$;
Zone II $U_{\text{total}} = U_{\text{incident}} + U_{\text{diffracted}}$;
Zone III $U_{\text{total}} = U_{\text{diffracted}}$;
Zone IV $U_{\text{total}} = U_{\text{diffracted}} + U_{\text{transmitted}}$.

Each geometrical optics (GO) field is discontinuous when crossing the related shadow boundary, but this discontinuity is compensated by an antisymetrical discontinuity of the diffracted field. Thus, the total field is continuous all around the wedge.

We remind the expression of the diffracted field in the space around the wedge as

$$U_d(P) = DU_i(Q)\sqrt{\frac{\rho}{s(\rho+1)}}\,e^{-jk_o s} \tag{1}$$

ρ is the caustic distance, s the observation distance, and D the diffraction coefficient given by [1] as

$$\begin{aligned} D_{\binom{s}{h}} &= D_1(\varphi-\varphi') + D_2(\varphi-\varphi') \\ &\quad + \left(R_{\binom{sn}{hn}} D_3(\varphi+\varphi') + R_{\binom{so}{ho}} D_4(\varphi+\varphi')\right). \end{aligned} \tag{2}$$

To keep continuity of the total field in case of a lossy dielectric wedges, we add two terms to the usual four-terms diffraction coefficient. These introduce two finite discontinuities, which compensate on each shadow boundary, those of the GO fields. Thus, the new six-terms diffraction coefficient is now expressed as

$$\begin{aligned} D_{\binom{s}{h}} &= D_1(\varphi-\varphi') + D_2(\varphi-\varphi') \\ &\quad + \left(R_{\binom{sn}{hn}} D_3(\varphi+\varphi') + R_{\binom{so}{ho}} D_4(\varphi+\varphi')\right) \\ &\quad + \left(\left[1+R_{\binom{sn}{hn}}\right]\left[1+R_{\binom{s2n}{h2n}}\right] D_5 \right. \\ &\quad \left. + \left[1+R_{\binom{so}{ho}}\right]\left[1+R_{\binom{s2o}{h2o}}\right] D_6\right). \end{aligned} \tag{3}$$

$R_{(s)}$ and $R_{(h)}$ are the reflection coefficients, respectively, in TE(soft) or TM(hard) polarization cases. When the wave penetrates from air into the dielectric, the reflection coefficient in TE polarization is given by

$$R_{(s)}(\theta_1) = \frac{\sin(\theta_1) - \sqrt{\underline{\epsilon}_r - \cos^2(\theta_1)}}{\sin(\theta_1) + \sqrt{\underline{\epsilon}_r - \cos^2(\theta_1)}}. \tag{4}$$

In this case, we have $R_{(sn)} = R_{(s)}(n\pi - \varphi')$ and $R_{(so)} = R_{(s)}(\varphi')$.

On the other interface (dielectric/air), it is given by

$$\begin{aligned} R_{(s2)}(\theta_2) &= \frac{\cos(\theta_2) - \sqrt{1/\underline{\epsilon}_r - \sin^2(\theta_2)}}{\cos(\theta_2) + \sqrt{1/\underline{\epsilon}_r - \sin^2(\theta_2)}} \\ R_{(s2n)} &= R_{(s2)}\left(\alpha - \arcsin\left(\frac{\cos(n\pi-\varphi')}{\sqrt{\epsilon_r}}\right)\right) \quad \text{and} \\ R_{(s2o)} &= R_{(s2)}\left(\alpha - \arcsin\left(\frac{\cos(\varphi')}{\sqrt{\epsilon_r}}\right)\right). \end{aligned} \tag{5}$$

The diffraction coefficients D_1, D_2, D_3, and D_4 are defined by [1] and [5] as

$$\begin{aligned} D_i(\varphi\pm\varphi') &= \frac{-e^{-j(\pi/4)}}{2n\sqrt{2\pi k_o}} \cot\left[\frac{\pi \pm (\varphi+\varphi')}{2n}\right] \\ &\quad \cdot F[k_o L a^{\pm}(\varphi\pm\varphi'). \end{aligned} \tag{6}$$

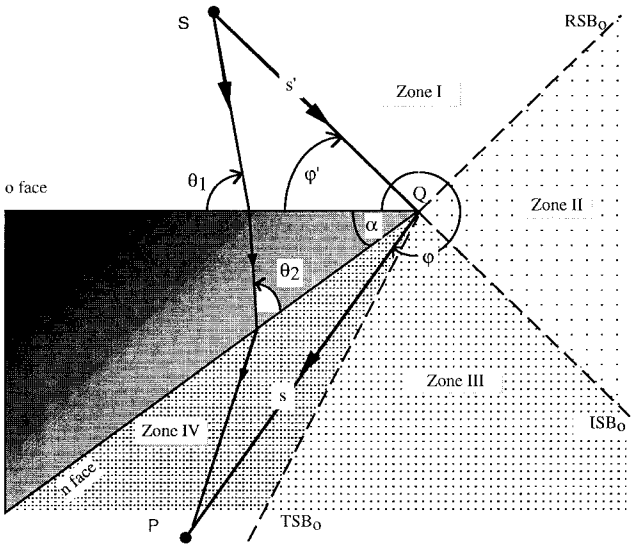

Fig. 1. Dielectric wedge geometry.

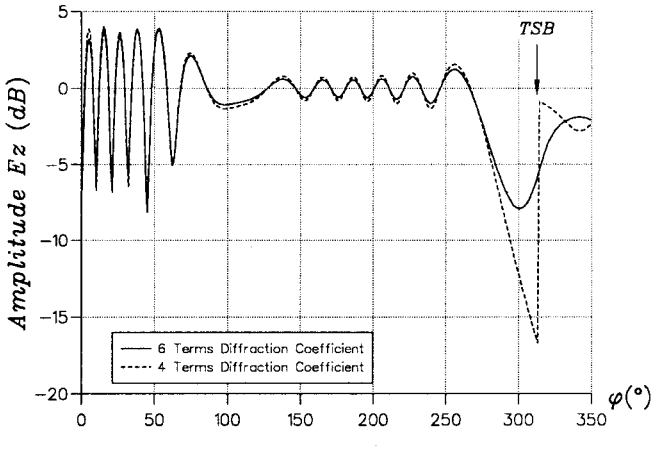

Fig. 2. Continuity of total UTD field with six-terms diffraction coefficient and comparison with the classical one (four terms). $f = 900$ MHz, $\varphi' = 105°$, $s = 1$ m, $\alpha = 10°$, $\epsilon_r = 10$, $\sigma = 0.001$ S/m.

Respectively, they ensure the continuity of the total field when crossing the ISB_n, the ISB_o, the RSB_n, and the RSB_o, but cannot compensate the discontinuity caused by the transmitted field on the TSB. Thus, the total field around a dielectric wedge, whose characteristics are given on Fig. 2, is clearly discontinuous on this shadow boundary when using the four-terms diffraction coefficient (2).

In (3), the two additional terms D_5 and D_6 allow ones to compensate the discontinuity created by the transmitted field, respectively, on the TSB_n and the TSB_o. According to the heuristic formulation given in [5], D_3 and D_4 are weighted by the reflection coefficients on o face and n face, respectively. In the same way, D_5 and D_6, which are related to the transmitted field, are weighted by the transmission coefficients of each dielectric interface

$$\left(1+R_{\binom{sn}{hn}}\right)\left(1+R_{\binom{s2n}{h2n}}\right) \quad \text{for } D_5 \quad \text{and}$$
$$\left(1+R_{\binom{so}{ho}}\right)\left(1+R_{\binom{s2o}{h2o}}\right) \quad \text{for } D_6.$$

Similarly to D_3, we can write D_5 as

$$D_5 = \frac{-e^{-j(\pi/4)}}{2n\sqrt{2\pi k_r}} \cot\left[\frac{-gn(\varphi')-\varphi}{2n}\right] F[k_r L^i a_5(g_n(\varphi'))]. \tag{7}$$

- $g_n(\varphi')$ defines the TSB_n calculated by applying the refraction Snell–Descartes law successively on the two interfaces air/dielectric and dielectric/air at the diffraction point Q

$$g_n(\varphi') = \frac{\pi}{2} - \arcsin\left\{\sqrt{\epsilon_r}\,\sin \cdot \left[\alpha - \arcsin\left(\frac{\cos(\alpha+\varphi')}{\sqrt{\epsilon_r}}\right)\right]\right\}. \tag{8}$$

- $$a_5(g_n(\varphi')) = 2\,\cos^2\left\{\frac{2\pi n N_5 + [\varphi + (\pi + g_n(\varphi'))]}{2}\right\}. \tag{9}$$

- N_5 is the nearest integer solution of

$$2\pi n N_5 + (\varphi + g_n(\varphi')) = 0. \tag{10}$$

The expressions a_6 and N_6 are deduced from those of a_5 and N_5 by changing into $g_n(\varphi')$ into $g_o(\varphi')$, which defines the TSB_o

$$g_o(\varphi') = \frac{3\pi}{2} - \alpha - \arcsin\left\{\sqrt{\epsilon_r}\,\sin \cdot \left[\arcsin\left(\frac{\cos(\varphi')}{\sqrt{\epsilon_r}}\right) - \alpha\right]\right\}. \tag{11}$$

- $$a_6(g_o(\varphi')) = 2\,\cos^2\left\{\frac{2\pi n N_6 + [\varphi - (\pi + g_o(\varphi'))]}{2}\right\}. \tag{12}$$

- N_6 is the nearest integer solution of

$$2\pi n N_6 + (\varphi - g_o(\varphi')) = 0. \tag{13}$$

Then we can write D_6 similarly to D_4 as

$$D_6 = \frac{-e^{-j(\pi/4)}}{2n\sqrt{2\pi k_r}} \cot\left[\frac{-g_o(\varphi')+\varphi}{2n}\right] F[k_r L^i a_6(g_o(\varphi'))]. \tag{14}$$

In Fig. 2, the improvement due to the new six-terms diffraction coefficient can be seen for $275° < j < 325°$. Indeed, the discontinuity observed for $\varphi = g_o(\varphi' = 105°) = 313{,}33°$ (TSB) on the dashed lines disappears once the two D_5 and D_6 terms are added to the diffraction coefficient.

III. Comparison Between UTD and FDTD in Case of a Single Wedge

Whereas ray methods like GTD and its extensions are based on locality of the scattering sources, numerical methods make the direct computation of the globally scattered field of a finite body. Consequently, there are two ways of comparing results given by both methods. First, one would consist in computing the global field scattered by a finite object by summing up all the ray contributions, but interpretation of the differences may then be cumbersome. Instead, the approach we have retained here is trying to isolate inside a numerical method the edge or wedge diffraction, while keeping the geometrical parameters as general as possible.

As UTD is used for a 2-D problem, we also use FDTD in two dimensions on a cylinder with triangular basis, with the goal of isolating one wedge diffraction illuminated by a plane wave. We implement Yee's leapfrog algorithm [10] with Mur second-order absorbing conditions and Taflove's corner ones [11]. Dielectric losses of material are taken into account conventionally through real electric conductivities. The incident pulse has Rayleigh like spectrum and is centered

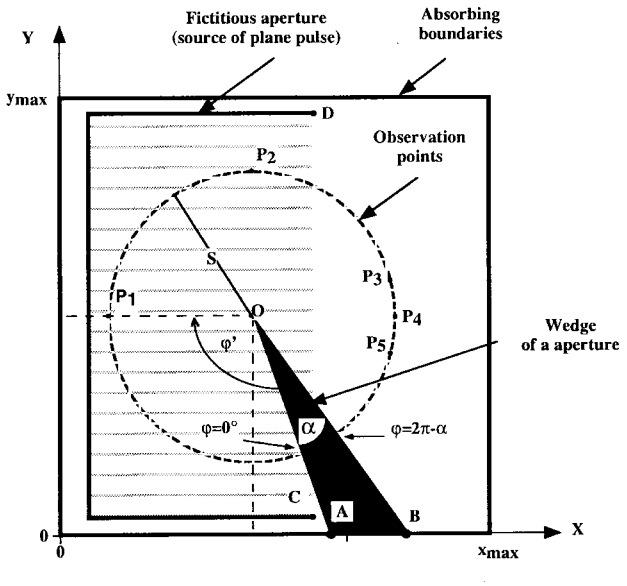

Fig. 3. Grid of FDTD calculation.

about 900 MHz. The base of the triangle rests on the Mur absorbing boundaries that have been adapted here and, along them, no significant spurious reflections were found at the junction of free-space and dielectric (Fig. 3). Because we want to isolate only one wedge diffraction, the concept of Huyghens surface for plane wave initialization is impossible to implement here. So we launch the plane pulse from a fictitious aperture CD (see Fig. 3) and improve the Mur absorbing boundaries by adding broad-band tapered radar-absorbing material (RAM) .

By studying the propagation of the incident pulse inside the calculation domain, we can observe that if we choose both an adapted time window and size of calculation domain, we do not observe any spurious reflections generated by the fictitious aperture CD. For this we choose the origin of the time on the vertical axe OP_2 and the propagation takes place according to the horizontal direction. It may be seen in Fig. 4 that at P_1 the pulse is delayed for 3.3 ns corresponding to the distance $OP_1 = 1$ m, and 6.6 ns later we observe an other smaller pulse corresponding to the reflection on the top of the wedge. The point P_4 located on the incident shadow boundary is illuminated by the pulse after this has been diffracted at O. Then we observe it at 3.3 ns with a very attenuated amplitude. For all the observation points, we observe only the diffraction and reflection phenomena of the pulse. Otherwise, the signal is quite flat during all the time analysis, which proves that no spurious reflection is observed.

After having reduced all spurious reflections to negligible levels, we validate our FDTD calculation domain by comparing results in a perfectly conducting case. The wedge (Fig. 3) of aperture α and tip O is illuminated on its OA face by a TE_z plane wave at 900 MHz impinging from $\varphi' = 105°$. For such a value of φ' the geometrical optics shadow boundaries are $RSB_o = 75°$ and $ISB_o = 285°$. The observation points (s, φ) are located on a circle centered at O and of radius $s = 1$ m. A fast Fourier transformation on FDTD results and a normalization by the frequency spectrum of the incident

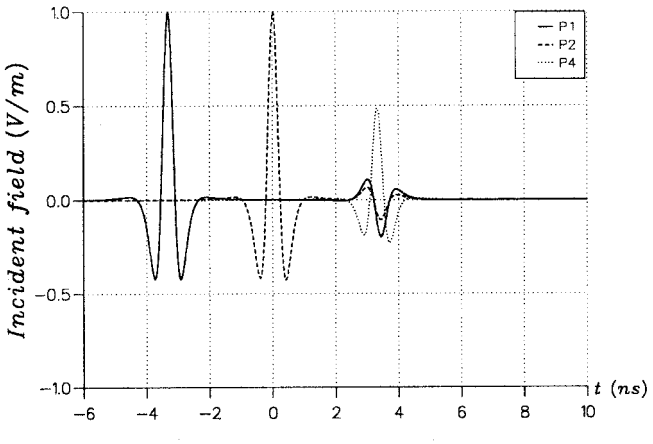

Fig. 4. Observation points (P_1, P_2, P_4).

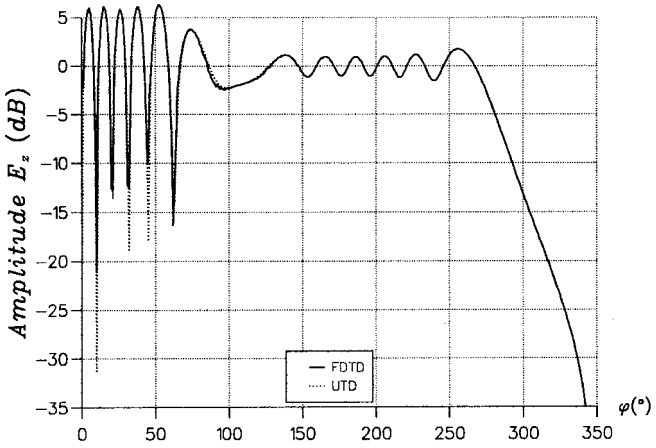

Fig. 5. Metallic wedge. $f = 900$ MHz, $\varphi' = 105°$, $s = 1$ m, $\alpha = 10°$.

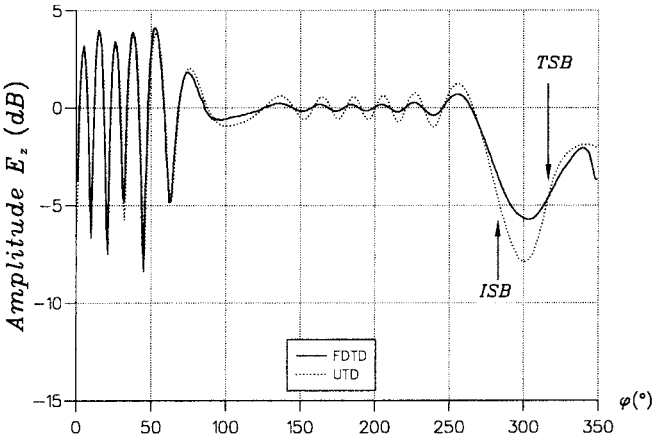

Fig. 6. Dielectric wedge. $f = 900$ MHz, $\varphi' = 105°$, $s = 1$ m, $\alpha = 10°$, $\epsilon_r = 0.001$ S/m.

Rayleigh pulse are performed to compare with UTD results in the frequency domain. We can check in Fig. 5 that agreement between the two methods is excellent.

To demonstrate the effectiveness of the UTD six-terms diffraction coefficient, we present (in Fig. 6) the results ob-

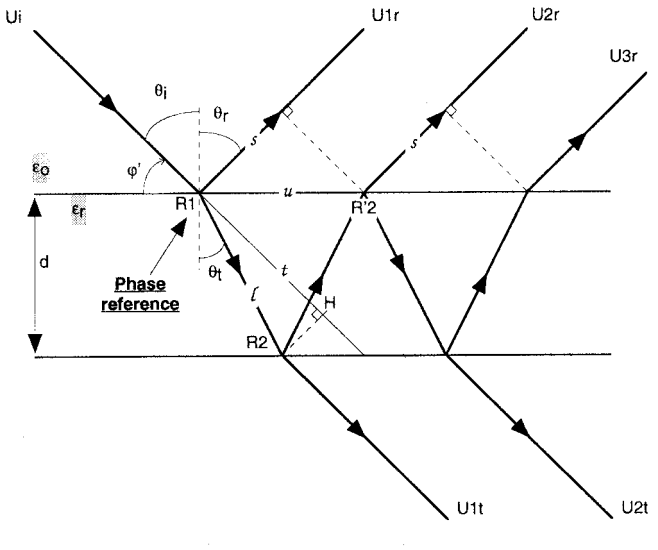

Fig. 7. Illustration of reflection and transmission on thin dielectric slab.

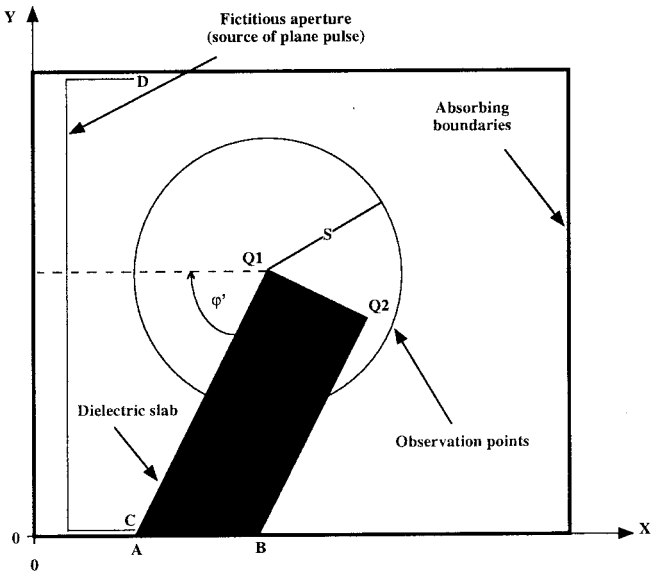

Fig. 8. FDTD modeling of the dielectric half-plane.

tained on a dielectric wedge by comparison with the FDTD method. The TSB depends on material properties and apex angle and is determined from (10). A good agreement between UTD and FDTD is obtained as a whole although differences are observed when diffraction is the only contribution to the total field (between ISB and TSB). As soon as GO field exists the agreement is quite good. In [12], we showed that whatever the value of the permittivity the differences between the two methods do not exceed 0.5 dB. These one observed between the ISB and the TSB can be explained by the heuristic nature of the diffraction coefficients. Moreover, the UTD doesn't take into account multipaths between the two dielectric interfaces which are calculated in the full wave FDTD approach.

IV. Study of a Thin Dielectric Half-Plane with Multiple Reflections

Because of the difficulty in UTD to implement the multiple reflections in the case of a dielectric wedge, we assess their influence in the more simple case of a dielectric slab using both FDTD and UTD. In this way, we can have an easier physical interpretation of the problem.

Consider the geometry of Fig. 7 showing a dielectric slab of thickness d illuminated by an incident field U_i. In [5], the expression of the incident reflected, diffracted, and transmitted fields can be found. They depend on multiple reflection and transmission coefficients that take the place of the single reflection and transmission coefficients previously used in the case of a dielectric wedge. Since the ISB and the TSB are similar, here we use a four-terms formulation for the UTD diffraction coefficient in which the reflection and transmission coefficients are derived from an infinite sum of terms related to each path inside the slab. From [5], the total layer reflection and transmission coefficients are

$$R_{mult} = \frac{R(\varphi')(1 - e^{-2jk_r l} e^{2jk_o l \sin(\theta_i)\sin(\theta_t)})}{1 - R^2(\varphi') e^{-2jk_r l} e^{2jk_o l \sin(\theta_i)\sin(\theta_t)}} \quad \text{and} \quad (15)$$

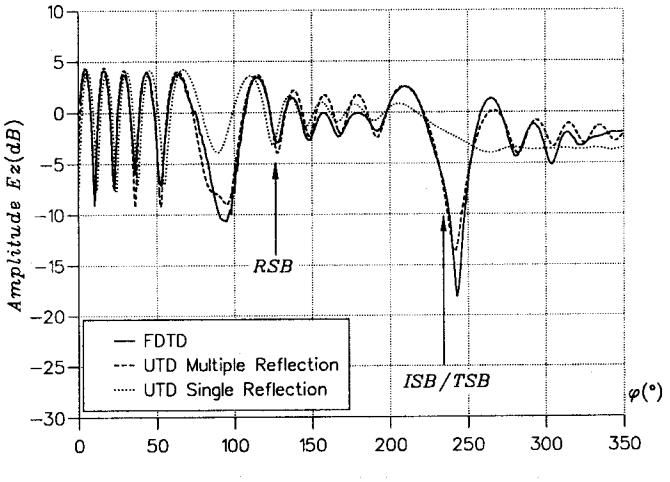

Fig. 9. UTD/FDTD comparison using geometry shown in Fig. 8. $f = 900$ MHz, $\varphi' = 55°$, $Q_1Q_2 = 10$ cm, $\epsilon_r = 10$, $\sigma = 0.001$ S/m.

$$T_{mult} = \frac{(1 - R(\varphi'))e^{-jk_r l} e^{jk_o t}}{1 - R^2(\varphi') e^{-2jk_r l} e^{2jk_o l \sin(\theta_i)\sin(\theta_t)}}. \quad (16)$$

$R(\varphi')$ is the single reflection coefficient from (4).

Thus, the diffraction coefficient D is calculated by

$$D = (1 - T_{mult}) D_{(\varphi - \varphi')} + R_{mult} D_{(\varphi - \varphi')} \quad (17)$$

in which $D_{(\varphi \pm \varphi')}$ id given by (6).

In UTD, we treat this problem by using this theory applied on an infinite half-plane. That is possible only if the thickness d of the slab is small enough to consider than ISB and TSB are the same.

In Fig. 8, we represent the geometry used in FDTD. The slab of thickness $d = Q_1Q_2$ is illuminated on its Q_1A face by a TE_z plane wave at 900 MHz impinging from $\varphi' = 55°$. The observation points P are located on a circle centered at O and of radius $s = 1$ m.

Results presented on Fig. 9 are quite convincing: as soon as we use a UTD formulation taking into account multiple reflec-

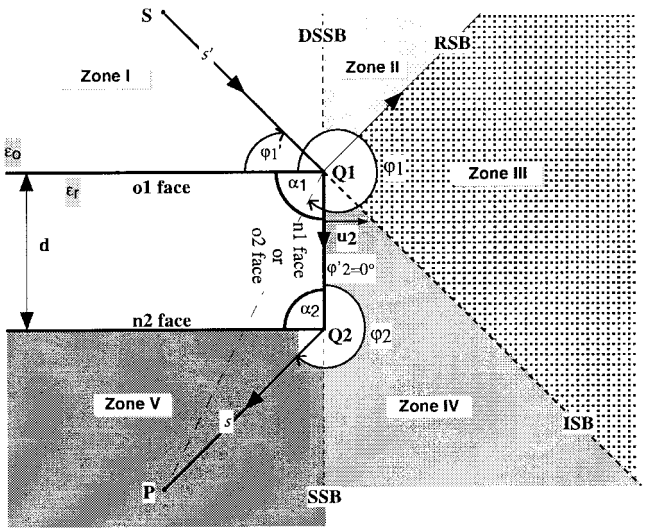

Fig. 10. Geometry of the diffraction by two consecutive wedges.

tions, the agreement with the FDTD is very good. Otherwise, if we use only the single reflection coefficient, differences of about 5 dB appear once the reflected and the incident fields disappear.

V. Study of a Thick Dielectric Half-Plane with Double Reflection

Even if we use multiple reflections, it remains small differences (1–2 dB) after the ISB inside the shadow boundary in Zone V (Fig. 10). That's why we introduce a second-order contribution, which is calculated using the slope diffraction. The latter allows one to find the doubly diffracted field by Q_1 and Q_2 in the shadow region. The expression of this new contribution is given by [7] as

$$E_2^{dd}(P) = \left[E_2^i(Q_2)D_2 + \frac{1}{2jk_o}\,\frac{\partial D_2}{\partial \varphi_2'}\,\frac{\partial E_2^i(Q_2)}{\partial u_2}\right] \cdot \sqrt{\frac{s'+d}{s(s+s'+d)}}\; e^{-jk_o s} \tag{18}$$

with

$$E_2^i(Q_2) = [E_1^i(Q_1)D_1]\sqrt{\frac{s'}{d(s'+d)}}\; e^{-jk_o d}. \tag{19}$$

The expressions of the two diffraction coefficients D_1 and D_2 are developed in [7].

On Fig. 10 for an incident wave on the $o1$ face, the space around the slab can be split into five areas limited by the double scattered shadow boundary (DSSB), the RSB, the ISB and the scattered shadow boundary (SSB). In each area the following fields exist:

Zone I $U_{\text{total}} = U_{\text{reflected}} + U_{\text{incident}} + U_{\text{diffracted}}$;
Zone II $U_{\text{total}} = U_{\text{reflected}} + U_{\text{incident}} + U_{\text{diffracted}} + U_{\text{doubly-diffracted}}$;
Zone III $U_{\text{total}} = U_{\text{incident}} + U_{\text{diffracted}} + U_{\text{doubly-diffracted}}$;
Zone IV $U_{\text{total}} = U_{\text{diffracted}} + U_{\text{doubly-diffracted}}$;
Zone V $U_{\text{total}} = U_{\text{doubly-diffracted}}$.

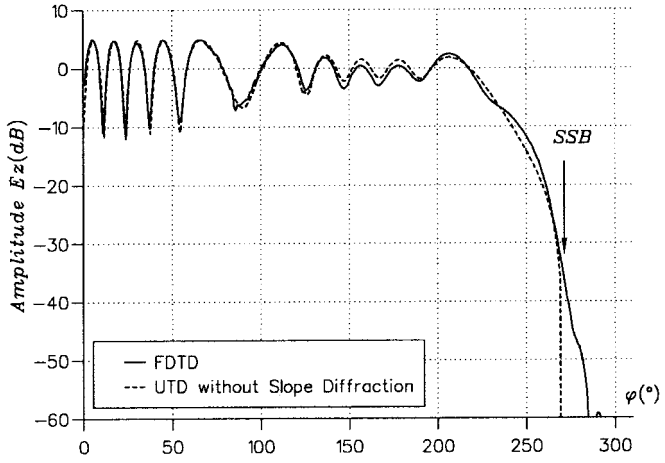

(a)

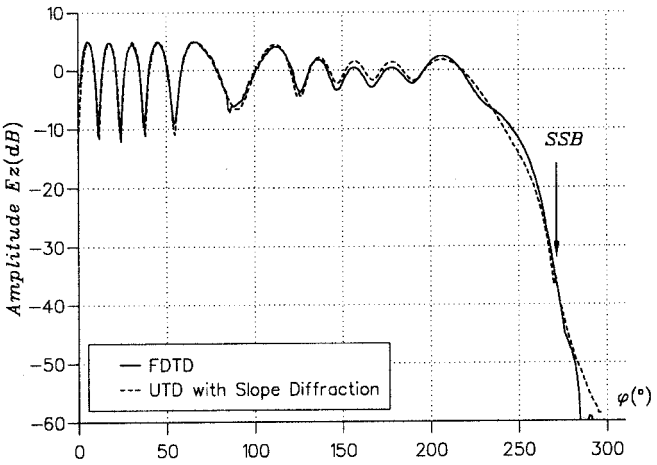

(b)

Fig. 11. UTD/FDTD comparison using geometry shown in Figs. 8 and 10. $f = 900$ MHz, $\varphi' = 55°$, $s = 1$ m, $Q_1Q_2 = 90$ cm, $\epsilon_r = 10$, $\sigma = 1$ S/m. (a) FDTD versus UTD without slope diffraction. (b) FDTD versus UTD with slope diffraction.

To calculate such a geometry, we now have to apply the UTD, not on an infinite half-plane as in the case of the slab, but on two consecutive wedge vertices. Indeed, the slope diffraction coefficient has been developed for a sufficient separation distance between these two consecutive wedges. This case is different from the case of an infinite half-plane because the ISB and the TSB cannot be merged here due to the thickness of the structure. Furthermore, in order to minimize the transmitted field and to keep the assumptions of the application domain of the slope diffraction coefficient, we choose a high lossy dielectric ($\sigma = 1$ S/m) and a large thickness $d = Q_1Q_2 = 90$ cm.

The results presented on Fig. 11(a) show a good agreement between UTD and FDTD for modeling the diffraction by two dielectric consecutive wedges before the SSB. Indeed, the only field calculated after the ISB is the diffracted field by Q_1 whose propagation is limited by the $o2$ face of the structure. Furthermore, for predicting the field all around the slab even in Zone V, we had to take into account the doubly diffracted field by Q_1 and Q_2 [Fig. 11(b)]. It's the only field present

in this zone. Thus, the results are quite good in all the space around the structure.

VI. Conclusion

An improvement of the UTD diffraction coefficient for the case of a lossy dielectric wedge has been presented. It allows one to consider the transmitted field through the structure by adding two new terms in the classical formulation of the diffraction coefficient. This new diffraction coefficient has been validated by a comparison with FDTD. In order to model exactly the same structure with these two methods, we previously adapted the FDTD time window and its calculation domain to isolate only one edge diffraction. Then we obtain a quite good agreement between the two methods. Small differences exist between the ISB and the TSB because we haven't taken into account multipaths inside the dielectric wedge. Thus, by implementing UTD and FDTD in the case of a thin dielectric slab, we have shown that multiple reflections inside the dielectric structure should be taken into account for a good agreement between UTD and a full wave approach such as FDTD. Finally, when losses are so important that the transmitted field doesn't exist, we have shown that it's possible to predict properly the field behind a thick dielectric slab by taking into account a slope diffraction coefficient generating the doubly diffracted field.

Note that in all our comparisons, typical UTD computation time are 0.01s on a HP735 work station against about 15 mn on a CRAY computer for FDTD. Thus, the UTD applied on dielectric structures is a very convenient method, fast and accurate, to calculate propagation in an urban environment.

Some more improvement could be achieved as the implementation of both transmission and slope transmission. Finally, we expect a further validation of our theoretical study from a comparison of all the results presented here with measurements.

Acknowledgment

The authors would like to thank M. Jaureguy and P. Borderies of ONERA-CERT for providing the FDTD code.

References

[1] R. G. Kouyoumjian and P. H. Pathak, "A uniform geometrical theory of diffraction for an edge in a perfectly conducting surface," *Proc. IEEE*, vol. 62, pp. 1448–1461, Nov. 1974.

[2] G. D. Maliuzhinets, "Excitation, reflection and emission of surface waves from a wedge with given face impedances," *Soviet Phys. Dokl.*, vol. 3, pp. 752–755, 1959.

[3] R. G. Rojas, "Electromagnetic diffraction of an obliquely incident plane wave field by a wedge with impedance faces," *IEEE Trans. Antennas Propagat.*, vol. 36, pp. 956–970, July 1988.

[4] R. Tiberio, G. Pelosi, and G. Manara, "A uniform GTD formulation for the diffraction by a wedge with impedance faces," *IEEE Trans. Antennas Propagat.*, vol. AP-33, pp. 867–873, Aug. 1985.

[5] W. D. Burnside and K. W. Burgener, "High frequency scattering by a thin lossless dielectric slab," *IEEE Trans. Antennas Propagat.*, vol. AP-31, pp. 104–110, Jan. 1983.

[6] R. J. Luebbers, "Finite conductivity uniform GTD versus knife edge diffraction in prediction of propagation path loss," *IEEE Trans. Antennas Propagat.*, vol. AP-32, pp. 70–76, Jan. 1984.

[7] ——, "A heuristic UTD slope diffraction coefficient for rough lossy wedges," *IEEE Trans. Antennas Propagat.*, vol. 37, pp. 206–211, Feb. 1989.

[8] G. Stratis, V. Anantha, and A. Taflove, "Numerical calculation of diffraction coefficients of generic conducting and dielectric wedges using FDTD," *IEEE Trans. Antennas Propagat.*, vol. 45, pp. 1525–1529, Oct. 1997.

[9] J. F. Rouviere, N. Douchin, and P. F. Combes, "Improvement of the UTD formulation for diffraction of an electromagnetic wave by a dielectric wedge," *Electron. Lett.*, vol. 33, no. 5, Feb. 1997.

[10] K. S. Yee, "Numerical solution of initial boundary value problems involving Maxwell's equations in isotropic media," *IEEE Trans. Antennas Propagat.*, vol. AP-14, pp. 302–307, May 1966.

[11] M. Jaureguy and P. Borderies, "An efficient initialization method for FDTD computation of plane wave scattering," in *Proc. IEEE Antennas Propagat. Soc.*, Newport Beach, CA, June 1995, pp. 848–851.

[12] J. F. Rouviere, N. Douchin, P. Borderies, and P. F. Combes, "Comparison between FDTD and UTD for the two dimensional case of a lossy dielectric wedge," in *Proc. Inst. Elect. Eng. 10th Int. Conf. Antennas Propagat. ICAP*, Edinburgh, U.K., Apr. 1997, pp. 2.290–2.293.

Jean-François Rouviere was born in France in 1968. He received the Diplôme d'Etudes Approfondies (D.E.A.) and Ph.D. degrees in electronics/microwave from the Toulouse University, France in 1994 and 1997, respectively.

From 1994 to 1997, he was Ph.D. student at the Office National d'Etudes et de Recherches Aérospatiales (O.N.E.R.A.) Toulouse Center (C.E.R.T.), where he led a project on the modeling of the radioelectric propagation in urban environment in behalf of France Telecom. In 1998 he then joined SILICOM, a service company specializing in telecommunication engineering. He is currently involved in a wide-band European satellite project for the multimedia.

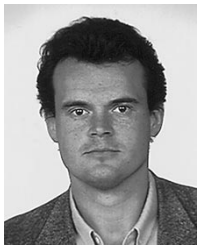

Nicolas Douchin was born in France in 1966. He received the Diplôme d'Ingénieur and the Diplôme d'Etudes Approfondies (D.E.A.) degrees from the Ecole Nationale Supérieure de l'Aéronautique et de l'Espace (SUPAERO), in 1989, and the Ph.D. degree in electronics from the same university, in 1992.

He spent six years as Research Engineer at the Office National d'Etudes et de Recherches Aérospatiales (O.N.E.R.A.), where his research activities focused on modeling radiowave propagation effects in various conditions including urban environments, the sea surface and the troposphere in which refraction and attenuation effects are observed. The aim of these research activities was to analyze the consequences of propagation effects on the performances of radar and telecommunication systems. Presently he is Head of the Telecommunication, Simulation, and Image Processing Group at CRIL INGENIERIE, Toulouse, France.

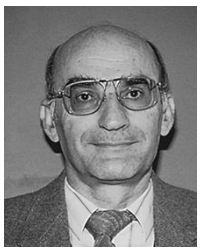

Paul F. Combes was born in France in 1943. He received the Doctorat de 3$^{\text{ième}}$ cycle from the Toulouse University, France, in 1968, and the Doctorat d'Etat es Sciences from the same university, in 1978

Since 1980, he has been a Professor of microwave engineering and Head of the Microwave Antennas and Devices Laboratory, Toulouse University. He is also in charge of the doctoral training in "microwave and optical telecommunication." He has been the thesis director of 26 theses and is actually conducting three theses. He is author or coauthor of about 100 publications covering the fields of reflector and array antennas, propagation of electromagnetic waves, radar, and radiometric and polarimetric devices for millimeter waves. In addition, he he is the author of 8 books, including *Microwaves Transmission for the Telecommunication* (New York: Wiley, 1991; 2nd ed., 1995), *Microwaves Components, Devices and Active Circuits* (New York: Wiley, 1987) and *Micro-Ondes : Lignes, Guides et Cavités—Volume 1* and *Micro-Ondes: Circuits Passifs, Propagation, Antennes—Volume 2* (Paris, France: Dunod, 1996, 1997, in French).